Tu A4 09

3D CSEM Inversion Of Data Affected by Infrastructure

J.P. Morten (EMGS), L. Berre* (EMGS), S. de la Kethulle de Ryhove (EMGS), V. Markhus (EMGS)

Summary

We consider the effect of metal infrastructure on marine 3D CSEM and the challenge from such responses in imaging. This is an issue for deployment of 3D CSEM in mature areas and for time-lapse production monitoring. We discuss the physical interaction between the imposed CSEM field and metallic structures. In a 3D CSEM inversion without special handling of the infrastructure responses, we demonstrate how the imaging artefacts complicate interpretation of the geology. Our data masking strategy shows how artefacts from a pipeline are effectively suppressed in a field data 3D inversion result. The modeling and imaging issues for metal well casing and metal pipelines are related, so our methodology applies in both cases.

Introduction

Application of 3D controlled-source electromagnetic (CSEM) resistivity mapping can significantly enhance exploration decisions, with a proven track-record in frontier areas. Increased interest to deploy 3D CSEM in more mature areas as well as for near-field exploration means that it will be more common to have metallic infrastructure such as well casing, pipelines, and subsea production systems located within the survey area. The imaging and characterization of resistive hydrocarbon reservoirs using 3D CSEM data relies on high-fidelity measurements that are used quantitatively in full waveform inversion. The total EM field includes not only the target resistor response, but also other components such as responses from metal infrastructure. The spatial scale and conductivity of the metal infrastructure is very different from geological resistivity variations, and in the inversion this can give imaging artefacts that complicate interpretation.

In this paper we consider the effect of metal infrastructure on 3D CSEM inversion results. Methods for accurate forward modeling of responses from steel casing in land CSEM data have recently been studied by several authors (Um et al. (2015), Tang et al. (2015), Puzyrev et al. (2016), Haber et al. (2016)). We focus on metal infrastructure effects in marine CSEM data. Our field data interpretation experience indicates that response from pipelines can both be of larger magnitude and affect larger parts of a survey dataset than that from casing from exploration drilling. We forward model the magnitude of this influence and omit the most affected data from the inversion input dataset. We show how such a data masking approach can suppress imaging artefacts from metal infrastructure responses without the requirement of detailed knowledge and representation of the steel infrastructure properties.

A metal infrastructure attribute for data masking

When infrastructure such as pipelines and well casing is present in the survey area, the imposed CSEM source field can lead to current channeling in the very conductive steel. This in turn leads to a change of the electromagnetic field which influences the measured total field response. In inversion we seek a resistivity model that reproduces the total field to within the measurement accuracy. Since the localized high-conductive regions can give rise to spatially extensive changes to the electromagnetic field with large magnitude, simply trying to invert the CSEM data as it is may lead to unrealistic model artefacts that make interpretation difficult. On the other hand, trying to represent both metre- and kilometre-scale variations in the same model leads to computational complexity issues. The large range in spatial scale implies that very fine discretization is required at least in parts of the model. The fine discretization requires large memory and CPU resources.

Effects from steel infrastructure responses can be suppressed by omitting the most affected data. Current 3D CSEM surveys result in large datasets where the subsurface response due to a given geological variation or target is captured by many observations. The inversion may then reconstruct the geological resistivity variations without an infrastructure effect from the reduced dataset. To enable this approach, we must determine the magnitude of the infrastructure response in each datum. We define the quantity χ_i that measures the significance of the infrastructure response by normalizing the complex response to the measurement uncertainty. The approach can then be described by the following,

$$\chi_i = \frac{\left| d_i^{\text{Infrastructure}} - d_i^{\text{Background}} \right|}{\delta d_i}, \qquad \text{Mask}\{d_i\} = \begin{cases} 0 \text{ if } \chi_i > t, \\ 1 \text{ else.} \end{cases} \tag{1}$$

Here we introduced d_i which is a component of the data vector $\mathbf{d}$ that includes the samples from all receivers, at all source-receiver combinations, and for all frequencies of the dataset. The denominator δd_i is the associated measurement uncertainty. The datasets $d_i^{\text{Infrastructure}}$ and $d_i^{\text{Background}}$ are simulated with and without steel infrastructure using the 3D finite-element approach described by Zhang and Key (2016). The unstructured mesh discretization allows to include both the small-scale features of well casings and pipelines as well as larger geological variations in the same model. An accurate resistivity model representing the area of a given field dataset, including resistors due to hydrocarbon reservoirs, may not be available. It is an assumption of this approach that a reasonable approximation to the metallic structure response $|d_i^{\text{Infrastructure}} - d_i^{\text{Background}}|$ can be obtained even without an accurate resistivity

model. The quantity χ_i specifies the spatial distribution and magnitude of metal infrastructure response. The map view in Figure 1(a) shows the pipeline response attribute for a shallow water dataset where a pipeline extends through the survey area. The distribution of the pipeline response is localized along the pipeline. The magnitude and extent is still not trivial to predict since this depends both on the source frequency and polarization as well as environmental parameters like water depth. The impact on inversion when standard settings are applied can be severe as shown by Figure 1(b) which is described in detail in section "3D inversion results". For this inversion the input data comprised the simulated pipeline responses in a homogeneous background. Both conductive and resistive artefacts are introduced by the inversion to attempt to explain the responses. In shallow water, the extensive and horizontally polar-

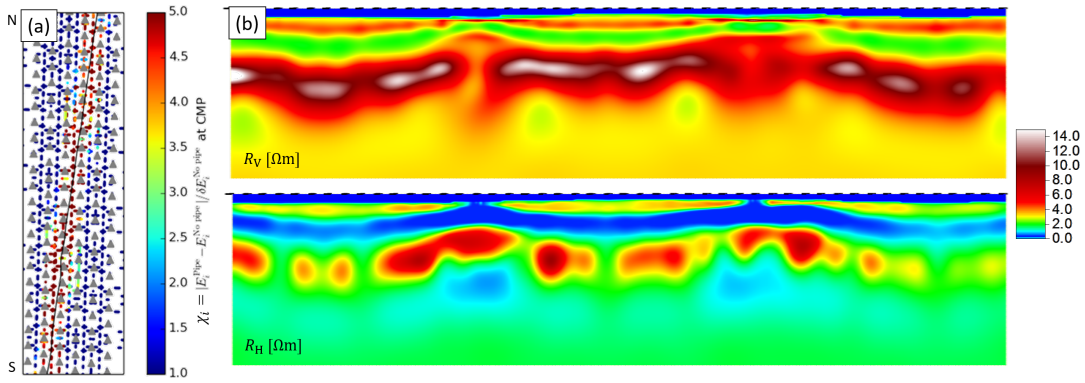

Figure 1 *(a) Pipeline attribute χ_i for 0.25 Hz electric field data in 5-6 km source-receiver offset plotted at CMP position, see Eq.* (1)*. Black line shows the pipeline, grey triangles show 3 km spaced receivers. (b) 3D inversion of pipeline response, section of vertical and horizontal resistivity along pipeline.*

ized airwave can interact strongly with the predominantly horizontally oriented pipeline, and produce a pipeline response even far away from the source. This shallow water interaction will be weaker for vertical steel well casing due to the orthogonality of the conductor and the airwave. The survey included source towlines in two orthogonal orientations. We find that inline data from the source towlines with an approximately orthogonal orientation with respect to the pipeline have less response from the pipeline than inline data from towlines approximately parallel to the pipeline. This is a result of coinciding polarization direction of the imposed field with the pipeline orientation (Hamilton et al., 2010).

We use the pipeline attribute defined above to create a dataset mask as shown by Eq. (1). The mask is used in data weights and when zero excludes the samples with the largest pipeline response from the inversion input dataset. We introduced the threshold parameter t that sets the upper limit of metal infrastructure response in included samples. A natural scale for t follows from assuming normal distributed measurement errors. The choice $t = 1$ corresponds to masking all data where the predicted infrastructure response exceeds one standard deviation. Conversely, we retain samples when the probability is 32 % or larger that the infrastructure response is less than random noise. The choice $t = 3$ includes more samples with measurable infrastructure response. In this case we keep the data even up to the point where the probability is small (0.3 %) that the steel infrastructure response is less than random noise effects. Keeping more data gives more artefacts in the inversion result, but at the same time may give better sensitivity to subsurface resistivity variations since more data is used in inversion.

3D inversion results

We consider pipeline effects in a 3D CSEM field dataset acquired in 2015 in the Norwegian Sea. A pipeline extends through the area approximately North to South. The survey included both North-South and East-West extending source towlines. The water depth is between 160 and 330 m. Interpretation of the 3D CSEM inversion results from the survey was hampered by imaging artefacts from the pipeline response. To demonstrate how such response can affect the imaging in a simple geology, we used the 0.25 Hz simulated dataset $d_i^{\text{Infrastructure}}$ of Eq. (1) as input to unconstrained 3D inversion. The pipeline was discretized with a triangular cross-section with an area corresponding to a 1 m radius circle. The pipeline conductivity was 10^6 S/m. The background model was a homogeneous half-space

with realistic bathymetry and 3.3 and 1.7 Ωm vertical and horizontal resistivity. The forward modeling software in the inversion used a finite-difference approach, and the domain was discretized as a regular grid with cell size 200 m×200 m×40 m. In Figure 1(b) we show a vertical section of the resulting resistivity model along the pipeline. We see that in order to fit the data, the inversion has introduced both resistive and conductive zones at depth. At points where the pipeline crosses the North-South oriented source towlines, the features are at more shallow depth. While the simple background model considered is insufficient for detailed comparisons to real data results, we note the general feature that resistive zones are "pulled up" at the pipeline-towline crossing positions. Such observations may be used as interpretation support when we consider artefacts in real data inversion results. In Figures 2 and

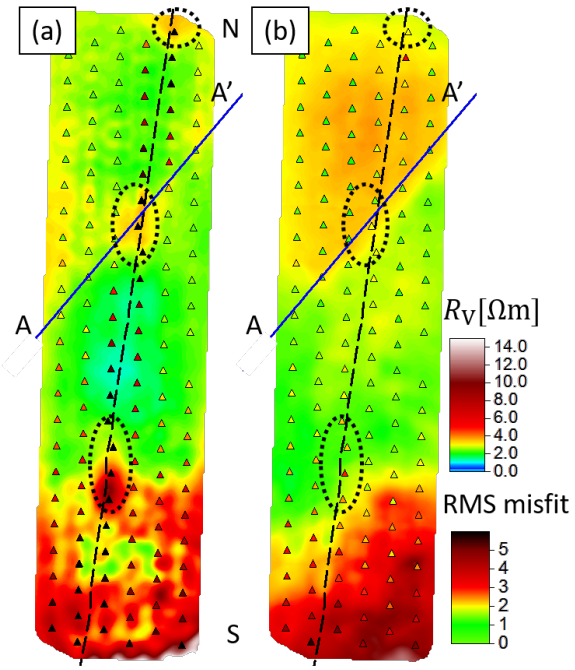

Figure 2 *Field data 3D CSEM vertical resistivity inversion results, depth section at 460 mBSL (a) without data masking and (b) masking pipeline affected data using $t = 3$ (same models as in Fig. 3). Plots show receiver positions (coloured triangles with black outline) and pipeline (black dashed line). Shallow resistors at towline/pipeline crossings in (a) are suppressed by masking in (b). The receiver indicators are color coded by root-mean-square (RMS) misfit in units of the standard deviation. The dataset included horizontal electric field responses at frequencies 0.125, 0.25, 0.5, 1.0 and 2.0 Hz. Plot (a) shows that residual data misfit is spatially correlated to the pipeline location. This shows how the inversion struggles to represent the metal infrastructure response. Misfit is increased in South part for both (a) and (b) where an escarpment of an identified stratigraphic layer has not been fully explained by the model.*

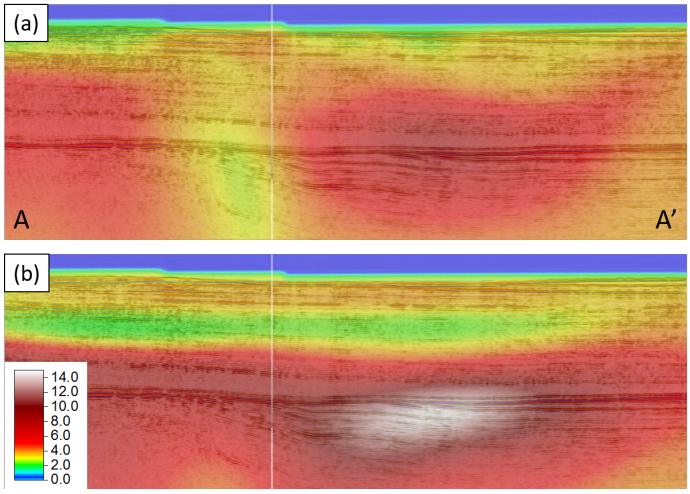

Figure 3 *Field data 3D CSEM vertical resistivity inversion results superimposed on 2D seismic. Plots show vertical sections along the line A-A' indicated in Fig. 2, the white vertical line marks the intersection with the pipeline. (a) No masking of pipeline-affected data. (b) Using the masking approach described by Eq. (1) with $t = 3$. The comparison shows that a shallow resistive and a deeper conductive artefact (a) have been suppressed by the masking in (b). We also see that a deeper resistor has been recovered more clearly in (b).*

3 we compare real data inversion results obtained with and without the pipeline response data masking approach described above and shown in Fig. 1(a). The result where the pipeline response affected data were included, shown in Figure 2(a), has resistive zones that spatially correlate with the points where the pipeline crosses a towline. We have highlighted these zones with dashed black ellipses in Figure 2. We note that the synthetic data inversion result shown in Figure 1 also exhibited such shallow resistive zones. In the inversion result obtained using masked input data, Figure 2(b), these resistive zones are absent. We remark that other resistors at the same depth are present in both results. Fig. 3 emphasizes how pipeline artefacts are suppressed while imaging of an interesting resistive feature (white colour)

coinciding with a seismic imaged pinch-out is improved by our masking approach. The result enhances the robustness of the interpretation of such resistors as real geological features and not artefacts.

Masking infrastructure-affected data allows to improve the quality of inversion images, but unfortunately also results in reduced sensitivity to subsurface structures. We can determine the magnitude and spatial extent of the sensitivity reduction by computing the trace over the data Hessian matrix to understand this effect. In cases where large parts of the data are masked away, the sensitivity loss can be severe. Therefore, we are currently implementing functionality for modelling metallic infrastructure in the fast and memory-efficient finite-difference forward modelling software used in our 3D inversion algorithms. The metal infrastructure response is then taken into account in the forward-modelled data, and this allows us to invert for data that include pipeline response and avoid the sensitivity reduction. We use the analytical solution of Wait (1952) to validate the accuracy of the forward modeling. We have also extended this solution to the case of hollow pipes, and find that depending on the specific combination of frequency, metal conductivity and pipe wall thickness, and in particular depending on the resulting skin depth in the metal, the induced current effect in the pipeline can be understood as either in a regime where (a) current flows through the entire metal cross-section; or (b) only a thin outer rim of the pipe wall cross-section effectively conducts current. For typical CSEM frequencies, pipe wall thicknesses and conductivities, both scenarios are possible. Imperfect knowledge of the pipeline parameters could lead to incorrect forward-modelled data. This problem can be overcome in an inversion approach with possibility to update the parameters representing the infrastructure.

Conclusions and acknowledgments

We consider the effect of metal infrastructure on marine 3D CSEM and the challenge from such responses in imaging. This is an issue for deployment of 3D CSEM in mature areas and in particular for development of CSEM time-lapse production monitoring. We discussed the physical interaction between the imposed CSEM field and metallic structures. In a 3D CSEM inversion without special handling of the infrastructure responses, we demonstrated how the imaging artefacts complicate interpretation of the geology. One way to remove such artefacts is to mask the input dataset samples where the metal infrastructure response exceeds a threshold. We present field data 3D inversion results that show how our approach reduces artefacts from a pipeline. The modeling and imaging issues for metal well casing and metal pipelines are related, so our methodology applies in both cases. Inversion of synthetic data including the pipeline responses provides interpretation support by showing how the imaging procedure represents the responses in a simple geology. The masking of metal infrastructure responses must be balanced with the reduction in subsurface geology sensitivity from the removal of data. We are currently developing an approach that fully incorporates metal infrastructure responses in a scheme suitable for large-scale 3D CSEM inversion. We thank EMGS for permission to publish this work.

References

Haber, E., Schwarzbach, C. and Shekhtman, R. [2016] Modeling electromagnetic fields in the presence of casing. *SEG Technical Program Expanded Abstracts 2016*, 959–964.

Hamilton, M.P., Mikkelsen, G., Poujardieu, R. and Price, A. [2010] CSEM Survey over the Frigg Gas Field, North Sea. *72nd EAGE Conference & Exhibition, Extended Abstracts, P074*.

Puzyrev, V., Vilamajo, E., Queralt, P., Ledo, J. and Marcuello, A. [2016] Three-Dimensional Modeling of the Casing Effect in Onshore Controlled-Source Electromagnetic Surveys. *Surveys in Geophysics*.

Tang, W., Li, Y., Swidinsky, A. and Liu, J. [2015] Three-dimensional controlled-source electromagnetic modelling with a well casing as a grounded source: a hybrid method of moments and finite element scheme. *Geophysical Prospecting*, **63**, 1491–1507.

Um, E.S., Commer, M., Newman, G.A. and Hoversten, G.M. [2015] Finite element modelling of transient electromagnetic fields near steel-cased wells. *Geophysical Journal International*, **202**, 901–913.

Wait, J.R. [1952] The cylindrical ore body in the presence of a cable carrying an oscillating current. *Geophysics*, **17**, 378–386.

Zhang, Y. and Key, K. [2016] MARE3DEM: A three-dimensional CSEM inversion based on a parallel adaptive finite element method using unstructured meshes. *SEG Technical Program Expanded Abstracts 2016*, 1009–1013.